Stroke amplifier for deformable mirrors

Robert H. Webb, Marc J. Albanese, Yaopeng Zhou, Thomas Bifano, and
Stephen A. Burns

We demonstrate a simple optical configuration that amplifies the usable stroke of a deformable mirror. By arranging for the wavefront to traverse the deformable mirror more than once, we correct it more than once. The experimental implementation of the idea demonstrates a doubling of 2.0 and 2.04 by two different means. © 2004 Optical Society of America

OCIS codes: 230.0230, 170.0170, 010.1080, 170.4460, 220.1000.

1. Introduction

The idea of correcting the existing aberrations of optical systems appeals to astronomers,[1] microscopists,[2] and vision scientists.[3–6] The use of adaptive optics to accomplish such a correction has had remarkable successes[7–9] and requires a wavefront sensor for assessing the aberrations in the light traversing the aberrating optics as well as a correcting device to adjust the wavefront.[10] Wavefront sensors typically operate by phase diversity (including shearing interferometers[11] and curvature sensors[12]) or local measurements of wavefront slopes (spatially resolved refractometer[13] and Shack–Hartmann wavefront sensor[14]). Correcting devices include devices such as spatial light phase modulators (liquid crystals[15]) and deformable mirrors,[16] which are the most common.[10]

In recent years deformable mirror technology has undergone rapid developments. Of special note is the development of MEMS (microelectromechanical) technology, which has the potential to produce lower-cost mirrors. Unfortunately, most commercial MEMS mirrors have only a limited stroke, or range of displacements. For vision, to correct a full range of ammetropia, we need 6 μm or more of stroke.[17] In astronomy cost is not a consideration and 5 μm of stroke is adequate, but for serious amateurs a 3-μm MEMS mirror might be affordable.

This paper demonstrates a simple optical configuration that amplifies the usable stroke in the deformable mirror (DM) on which adaptive optics depends. DMs consist typically of one to many actuators that change the position of a reflecting surface locally by a few micrometers. Ours has 140 actuators and a square aperture of 3.3 mm. Its stroke is 4 μm. If the actuator stroke is many micrometers (many wavelengths), then wavefronts with substantial distortion may be corrected. Commercially available DM's use actuators that are either piezoelectric or electrostatic devices, and it is difficult to achieve more than a few micrometers without greatly increased expense and complexity.

2. Amplifier Design

Figure 1 shows a design that allows the wavefront to pass twice over the DM surface, with proper alignment and phasing, so that the mirror's correction is impressed twice on the wavefront.

Here, for convenience in this tutorial, the input light is a collimated beam, so its wavefront is flat. It is convenient to put the wavefront sensor on the output beam, after the DM, though that is not necessary. After reflection from the DM the wavefront (wavefront 1) has an off-center mesa impressed on it, which leads the rest of the wavefront. (The mesa in the wavefront is twice the height of the mesa in the DM, but that is incidental to this argument.) Wavefront 1 propagates along the $-Z$ direction, with the mesa toward $-Z$, as is the mesa on the DM.

Then wavefront 1 is inverted in X and Y by the lens pair, so that wavefront 2 is shown with the mesa off center on the other side of the optic axis of the lenses,

R. H. Webb (webb@eri.harvard.edu) and S. A. Burns are with the Schepens Eye Research Institute, 20 Staniford Street, Boston, Massachusetts 02114. M. J. Albanese is with the Department of Electrical and Computer Engineering and Yaopeng Zhou is with the Department of Aerospace and Mechanical Engineering, Boston University, 110 Cummington Street, Boston, Massachusetts 02215. T. Bifano is with the Department of Manufacturing Engineering, Boston University, 15 Saint Mary's Street, Boston, Massachusetts 02215.

Received 28 January 2004; revised manuscript received 4 June 2004; accepted 7 June 2004.

0003-6935/04/285330-04$15.00/0

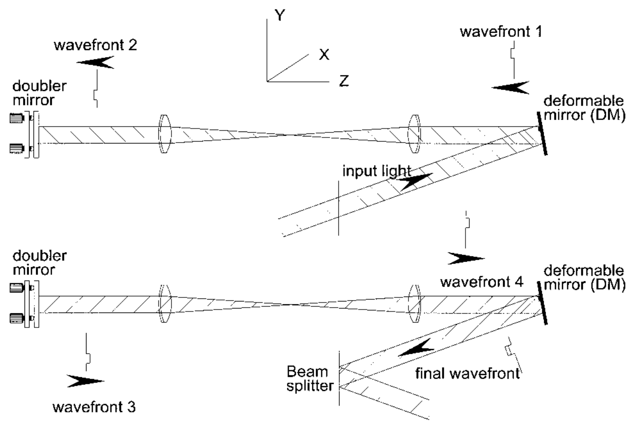

Fig. 1. Simple version of the amplifier. Light incident on the deformable mirror is returned with proper inversions so that an image of the DM lands exactly on the DM. The DM thus acts twice on the incident wavefront. A detailed discussion is presented in the text.

but the mesa is still toward $-Z$, thus still leading the rest of the wavefront. On reflection from the doubler mirror, wavefront 3 has the same XY orientation as wavefront 2, but the mesa is now toward $+Z$, so that it is again leading the rest of the wavefront, which is now moving toward $+Z$. Again the lenses flip the lateral orientation to wavefront 4, without changing the Z orientation. Wavefront 4 now exactly matches the DM in XY but is reversed in Z. Since the mesa on the wavefront gets to the mesa on the DM first, it is reflected first, and the final wavefront has a mesa on it twice the height of the mesa after one pass of the DM. Thus the effect of the DM's stroke has been doubled.

It is not necessary to start with a collimated beam, nor to use the focal lengths shown here. The critical adjustment in our implementation is that the doubler mirror be conjugate to the DM (an image of the DM falls on the doubler mirror). Imaging and reimaging by the lenses ensure that the wavefront returning to the DM has the correct size and orientation.

Figure 2 uses a shorthand in which the dots represent the focal points for the beams. Here the incident and corrected beams are separated by a small angle, so the beams to and from the doubler mirror are separated, as shown.

The doubler mirror in Fig. 2 is angled so that the final exiting beam is separated from the original incident beam. That configuration avoids the use

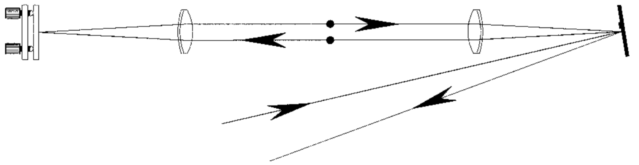

Fig. 2. Simplified schematic for a variant of Fig. 1. The filled circles represent focal points for the beams, shown here as single (chief) rays.

of a beam splitter to separate the incident and processed beams. We have used that arrangement, which serves to maximize the light efficiency, but the design with the beam splitter introduces no aberrations. The lenses (or mirrors) in the Fig. 2 variant are used slightly off axis, so they should be slow. We use 100-mm lenses for a 3-mm pupil. That means that 3 mm is the beam diameter at the DM and the doubler mirror and at the lenses for the collimated beam of the illustration. A separation angle of 2 deg lets the incident and exit beams be generously separated, and that means the separated beams traverse the lenses only 3.5 mm off axis. The resulting aberration, when good-quality achromats are used, is negligible (the system remains diffraction limited). To model this in ZEMAX[18] we put in the actual lenses we are using and incident collimated light. A focused beam then has its geometric (aberration controlled) spot radius as 34% of the Airy disk radius, or 0.2 wave peak-to-peak aberration. A separation of 0.5 deg is more typical for our implementation and still adequate for beam separation, but it gives no appreciable aberration, so we report the larger values. The critical constraint is that the doubler system reimage the DM on itself in essentially an aberration-free manner. While exact specifications will depend on the exact implementation, a value of an eighth-wave rms error is a reasonable constraint. This is readily achieved with the slow optics we are describing.

3. Uncollimated Beams

A more serious problem is that of lower-*f*-number beams. Modeling with a convergent or divergent beam is reassuring in that the amplifier still works as specified. However, eventually the size of the optics matters: Small optics will vignette a big beam. More importantly, a tilted lens or mirror will cause more aberration of a converging or diverging beam than of a collimated beam. Even an $f/10$ beam is bad news for a system with tilts and decenters. Luckily, those are not necessary with lenses in the configuration of Fig. 1, but, in the system with mirrors that we describe below, near collimation is required. The configuration of Fig. 2 with the lenses slightly decentered avoids the need of a beam splitter, but it too is happier close to collimation.

4. Confirming Experiment

To test the amplifier we created a local distortion of 3×3 actuators on the DM (Boston Micro Machines[19]) and observed the change in the Shack–Hartmann pattern. Figures 3 and 4 show two configurations used to test the amplifier. The basic configuration is that of Fig. 1, with the input and output beams collinear and a beam splitter to separate the corrected wavefront from the original. The variations allow a single pass over the DM, which is sensed by the Shack–Hartmann sensor and compared with the double pass of Fig. 1, with minimal changes to the configuration.

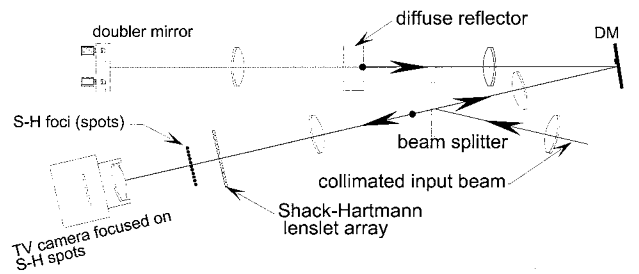

Fig. 3. The diffuse reflector at the focus acts as a point source. The resulting light retains no phase information from the incident beam and so makes a single pass over the DM, which is sensed by the Shack–Hartmann (S-H) sensor.

In the configuration of Fig. 3, the diffuse reflector acts as a point source. Here it is illuminated through the DM, but all that phase information is lost on diffuse reflection, so it could have been illuminated by a separate beam focused at the diffuse reflector. We used this configuration because we could go from Fig. 3 to Fig. 1 simply by removing the diffuse reflector. We confirmed that the diffuse reflector was located at the focal point of the lens by flattening the deformable mirror, testing that the resulting beam is collimated.

The second single-pass configuration is shown in Fig. 4. This differs from Fig. 1 merely by rotation of the DM. In Fig. 4 the DM is normal to the beam, sending it back on itself, while in Fig. 1 the DM angles the beam a bit to send it into the amplifier—and then back on itself.

The Shack–Hartmann spots form a basic square grid if the beam is collimated, and the spots move from that grid owing to the action of the DM. The spots move visibly more when the doubler is used, which turns out to be a simple and accurate method of alignment. Of course, the Shack–Hartmann sensor detects wavefront slopes, so it reads the mesa as a bump, not as a flat-topped structure. To quantify the changes, we measured the spot displacements at each lenslet (spot) within the Shack–Hartmann pupil. The actual data are these spot displacements, so we need not go so far as analyzing them to define slopes; we just use the raw data. The displacements are small, so we compare the rms averages: rms $= [\Sigma\,(\Delta x)^2/n]^{1/2}$, where the number of displacements n is 242 (two for each spot). We find that these ratios are

$$\begin{aligned}\text{rms (doubler)/rms (diffuser)} &= 1.3308/0.6521\\ &= 2.04,\\ \text{rms (doubler)/rms (single pass)} &= 1.4431/0.7209\\ &= 2.00.\end{aligned}$$

The two comparisons refer to the two different ways of generating the unamplified wavefront, as shown in Figs. 3 and 4. The diffusing reflector of Fig. 3 is placed at the first focus after the DM in Fig. 1, so that the single pass is from a point source, collimated by a lens, landing once on the DM. The diffuser scrambles the wavefront after its first pass over the DM. The wavefront mesa is readily apparent on the Shack–Hartmann display, and adjusting the DM alignment moves it so that all Shack–Hartmann lenslets are filled and the mesa is slightly off center, as it is on the DM itself. Then the diffuser is removed, and the mesa becomes twice as big. (That means that the spot displacements become twice as big.)

In the other comparison, shown in Fig. 4, the DM was turned so that only one pass was made. For convenience, the DM tilt was adjusted to place the mesa in the same part of the pupil as that used in the diffuser and amplifier measurements, although this is not required because the rms spot displacements are taken over the whole pupil of the Shack–Hartmann sensor.

5. Variants on the Basic Design

Some minor variants on the optical design make it even simpler. Both the lens pair and the mirror can be replaced with concave mirrors. Figure 5 replaces the flat doubler mirror and one of the relay lenses with a concave mirror, and the other relay lens with a second concave mirror. For tutorial convenience, all focal lengths are equal, but that is not necessary.

The advantages of the simple design with two mirrors are not just in the reduction in the number of elements. Mirrors are achromatic and cast no ghost images. Further, fine alignment depends only on tilts and axial positioners if the mirrors are reasonably confocal. We believe that the design

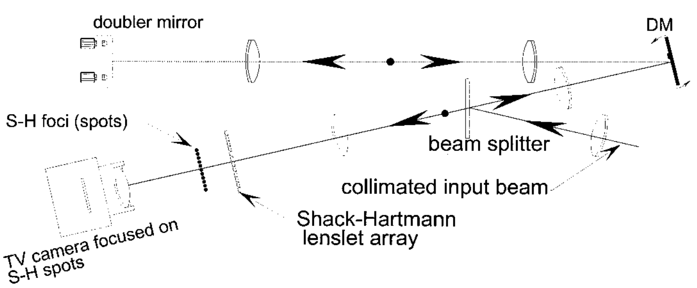

Fig. 4. For another single-pass configuration, we just turn the DM normal to the incident beam, so that it sends the light directly back to the Shack–Hartmann (S-H) sensor.

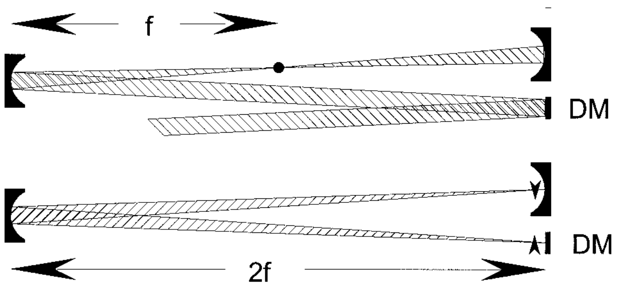

Fig. 5. Simplest arrangement of the amplifier. The concave mirrors are drawn to have the same focal lengths. The upper drawing shows how the collimated beam is recollimated by the doubler. The lower drawing demonstrates how the DM is reimaged on itself after proper inversions.

with all mirrors is the most convenient and tolerant, but it does require a nearly collimated beam. Spherical mirrors are entirely adequate for diffraction-limited performance as long as the angles are kept small. For the 4-deg tilts we use, the rms spot size is 54% of the Airy disk in a ZEMAX model, or a Strehl ratio of 0.82.[20,21]

6. Iterations of the Design

Of course, we can iterate the procedure to add more doublers and increase the stroke further. Using the configuration of Fig. 2, each doubler added simply adds another copy of the DM's effect. That is, we do not double the doubler. However, using a combination of the Figs. 1 and 2 configurations (one that requires a beam splitter and one that uses separation in angle), we do double the doubler.

It is important to note that too much doubling may cause noise problems. If the DM's surface is $f(x, y)$, there will be an inevitable uncertainty at each actuator position, say, $\Delta f(x, y)$. Doubling $f(x, y)$ doubles Δf, coherently. Quadrupling gives $4f(x, y)$ and $4\Delta f(x, y)$. If Δf is $\lambda/20$, then quadrupling makes the surface $\lambda/5$.

Practical limits dictate that one should not expect a DM to correct the aberrations introduced by the rest of the optics. Rather, it should be saved for correcting the time-varying portions of the system (for us the eye). In principle, system aberrations can be corrected by a stationary phase plate, once they are measured by the wavefront sensor.

This work was supported in part by grants R01 EY 14106 and R01 EY014375 from the National Eye Institute. Deformable mirrors used in this work were provided by Boston Micromachines Corporation.

References

1. M. C. Roggeman, B. M. Welsh, and R. Q. Fugate, "Improving the resolution of ground-based telescopes," Rev. Mod. Phys. **69,** 438–505 (1997).
2. M. A. A. Neil, R. Juskaitis, T. Wilson, Z. J. Laczik, and V. Sarafis, "Optimized pupil-plane filters for confocal microscope point-spread function engineering," Opt. Lett. **25,** 245–247 (2000).
3. N. Doble, G.-Y. Yoon, L. Chen, P. Bierden, B. Singer, S. Olivier, and D. R. Williams, "Use of a microelectromechanical mirror for adaptive optics in the human eye," Opt. Lett. **27,** 1537–1539 (2002).
4. E. J. Fernandez, I. Iglesias, and P. Artal, "Closed-loop adaptive optics in the human eye," Opt. Lett. **26,** 746–748 (2001).
5. L. J. Zhu, P. C. Sun, D. U. Bartsch, W. R. Freeman, and Y. Fainman, "Wave-front generation of Zernike polynomial modes with a micromachined membrane deformable mirror," Appl. Opt. **38,** 6019–6026 (1999).
6. L. N. Thibos and A. Bradley, "Use of liquid-crystal adaptive-optics to alter the refractive state of the eye," Optom. Vis. Sci. **74,** 581–587 (1997).
7. J. Liang, D. R. Williams, and D. T. Miller, "Supernormal vision and high-resolution retinal imaging through adaptive optics," J. Opt. Soc. Am. A **14,** 2884–2892 (1997).
8. A. Roorda, F. Romero-Borja, W. J. Donnelly, III, H. Queener, T. J. Hebert, and M. C. W. Campbell, "Adaptive optics scanning laser ophthalmoscopy," Opt. Express **10,** 405–412 (2002).
9. L. A. Thompson, "Adaptive optics in astronomy," Phys. Today 47(12), 24 (1994).
10. P. W. Milonni, "Resource letter: AOA-1: adaptive optics for astronomy," Am. J. Phys. **67,** 476–485 (1999).
11. M. P. Rimmer, "Method for evaluating lateral shearing interferograms," Appl. Opt. **13,** 623–629 (1974).
12. M. A. Van Dam and R. G. Lane, "Extended analysis of curvature sensing," J. Opt. Soc. Am. A **19,** 1390–1397 (2002).
13. R. H. Webb, C. M. Penney, J. Sobiech, P. R. Staver, and S. A. Burns, "The SRR: a null-seeking aberrometer," Appl. Opt. **42,** 736–744 (2003).
14. B. C. Platt and R. Shack, "History and principles of Shack–Hartmann wavefront sensing," J. Refr. Surg. **17,** S573–S577 (2001).
15. S. R. Dale, G. D. Love, R. M. Myers, and A. F. Naumov, "Wave-front correction using a self-referencing phase conjugation system based on a Zernike cell," Opt. Commun. **191,** 31–38 (2001).
16. T. Shirai, T. H. Barnes, and T. G. Haskell, "Adaptive wave-front correction by means of all-optical feedback interferometry," Opt. Lett. **25,** 773–775 (2000).
17. J. Porter, A. Guirao, I. Cox, and D. R. Williams, "Monochromatic aberrations of the human eye in a large population," J. Opt. Soc. Am. A **18,** 1793–1803 (2001).
18. ZEMAX Development Corporation, 4901 Morena Blvd., Suite 207, San Diego, Calif. 92117–7320.
19. Boston Micromachines Corporation, Watertown, Mass. 02472: Model μDM140 deformable mirror system.
20. S. Bara, T. Mancebo, and E. Moreno-Barriuso, "Positioning tolerances for phase plates compensating aberrations of the human eye," Appl. Opt. **39,** 3413–3420 (2000).
21. A. Guirao, D. R. Williams, and I. G. Cox, "Effect of rotation and translation on the expected benefit of an ideal method to correct the eye's higher-order aberrations," J. Opt. Soc. Am. A **18,** 1003–1015 (2001).